frontiers | Frontiers in Endocrinology

TYPE Original Research
PUBLISHED 07 November 2023
DOI 10.3389/fendo.2023.1273878

OPEN ACCESS

EDITED BY
Xiaoning Zhang,
Nantong University, China

REVIEWED BY
Luís Pedro Rato,
Instituto Politécnico da Guarda, Portugal
Tao Luo,
Nanchang University, China

*CORRESPONDENCE
Kun Li
likun@hmc.edu.cn
Yamei Xue
yameixue@zju.edu.cn

†PRESENT ADDRESS
Haifeng Xie,
Laboratory Medicine Center, Hangzhou Traditional Chinese Medicine (TCM) Hospital Affiliated to Zhejiang Chinese Medical University, Hangzhou, China

RECEIVED 07 August 2023
ACCEPTED 10 October 2023
PUBLISHED 07 November 2023

CITATION
Cheng X, Xie H, Xiong Y, Sun P, Xue Y and Li K (2023) Lipidomics profiles of human spermatozoa: insights into capacitation and acrosome reaction using UPLC-MS-based approach. *Front. Endocrinol.* 14:1273878. doi: 10.3389/fendo.2023.1273878

Lipidomics profiles of human spermatozoa: insights into capacitation and acrosome reaction using UPLC-MS-based approach

Xiaohong Cheng[1,2], Haifeng Xie[1†], Yuping Xiong[1,2], Peibei Sun[1], Yamei Xue[3*] and Kun Li[1,4*]

[1]School of Pharmacy, Hangzhou Medical College, Hangzhou, China, [2]School of Basic Medical Sciences and Forensic Medicine, Hangzhou Medical College, Hangzhou, Zhejiang, China, [3]Reproductive Medicine Center, Department of Obstetrics and Gynecology, Sir Run Run Shaw Hospital, College of Medicine, Zhejiang University, Hangzhou, Zhejiang, China, [4]Zhejiang Provincial Laboratory of Experimental Animal's & Nonclinical Laboratory Studies, Hangzhou Medical College, Hangzhou, Zhejiang, China

Introduction: Lipidomics elucidates the roles of lipids in both physiological and pathological processes, intersecting with many diseases and cellular functions. The maintenance of lipid homeostasis, essential for cell health, significantly influences the survival, maturation, and functionality of sperm during fertilization. While capacitation and the acrosome reaction, key processes before fertilization, involve substantial lipidomic alterations, a comprehensive understanding of the changes in human spermatozoa's lipidomic profiles during these processes remains unknown. This study aims to explicate global lipidomic changes during capacitation and the acrosome reaction in human sperm, employing an untargeted lipidomic strategy using ultra-performance liquid chromatography-mass spectrometry (UPLC-MS).

Methods: Twelve semen specimens, exceeding the WHO reference values for semen parameters, were collected. After discontinuous density gradient separation, sperm concentration was adjusted to 2 x 10^6 cells/ml and divided into three groups: uncapacitated, capacitated, and acrosome-reacted. UPLC-MS analysis was performed after lipid extraction from these groups. Spectral peak alignment and statistical analysis, using unsupervised principal component analysis (PCA), bidirectional orthogonal partial least squares discriminant analysis (O2PLS-DA) analysis, and supervised partial least-squares-latent structure discriminate analysis (PLS-DA), were employed to identify the most discriminative lipids.

Results: The 1176 lipid peaks overlapped across the twelve individuals in the uncapacitated, capacitated, and acrosome-reacted groups: 1180 peaks between the uncapacitated and capacitated groups, 1184 peaks between the uncapacitated and acrosome-reacted groups, and 1178 peaks between the capacitated and acrosome-reacted groups. The count of overlapping peaks varied among individuals, ranging from 739 to 963 across sperm samples. Moreover, 137 lipids had VIP values > 1.0 and twenty-two lipids had VIP > 1.5, based on the O2PLS-DA model. Furthermore, the identified twelve lipids encompassed increases in PI 44:10, LPS 20:4, LPA 20:5, and LPE 20:4, and

decreases in 16-phenyl-tetranor-PGE2, PC 40:6, PS 35:4, PA 29:1, 20-carboxy-LTB4, and 2-oxo-4-methylthio-butanoic acid.

Discussion: This study has been the first time to investigate the lipidomics profiles associated with acrosome reaction and capacitation in human sperm, utilizing UPLC-MS in conjunction with multivariate data analysis. These findings corroborate earlier discoveries on lipids during the acrosome reaction and unveil new metabolites. Furthermore, this research highlights the effective utility of UPLC-MS-based lipidomics for exploring diverse physiological states in sperm. This study offers novel insights into lipidomic changes associated with capacitation and the acrosome reaction in human sperm, which are closely related to male reproduction.

KEYWORDS

lipidomics, spermatozoa, capacitation, acrosome reaction, male reproduction, sperm function, 20-carboxy-LTB4, 2-oxo-4-methylthio-butanoic acid

Introduction

Lipidomics involves the comprehensive analysis and characterization of lipids and their systemic-level interactions (1). Lipidomics elucidates the physiological and pathological roles of lipid molecules across cellular, tissue, and organ levels and their interplay with various diseases via metabolic enzymes and signaling pathways. Lipidomics augments our understanding of membrane lipid regulation, encompassing elements such as fluidity, fusion, lipid rafts, cytoskeleton, kinases, and membrane proteins (2). Additionally, lipidomics has utility in biomarker screening, clinical trials (3, 4), and disease prognosis (5). Lipids play crucial roles in energy storage, cellular structure, and signaling, and maintaining lipid homeostasis is essential for overall health while lipid defects can contribute to pathogenesis and diseases (6, 7). In the context of reproductive biology, lipids are crucial for sperm survival, maturation, and proper functioning during fertilization (8, 9). Phospholipids, including phosphatidylcholine, phosphatidylethanolamine, phosphatidylinositol, and phosphatidylserine, are integral components of cell membranes and modulate membrane fluidity, ion channel activation, and the functionality of membrane-binding enzymes (10). Recent research has demonstrated correlations between lipidomic alterations in asthenozoospermic men and sperm motility (11).

Capacitation and the acrosome reaction are two essential sperm functions required for fertilization. Capacitation refers to the change enabling spermatozoa to acquire fertilizing capacity during the period of spermatozoa's exposure to the female reproductive tract (12). During capacitation, the sperm undergo the regulation from the complicated signal pathways involved in ion fluxes and kinase (13, 14). Meanwhile, the lipid composition and distribution of the sperm plasma membrane change, encompassing modifications in phospholipids, cholesterol, anionic lipids, lipid methylation, and lipid diffusion (15). When capacitated, sperm are competent to undergo the acrosome reaction. The acrosome reaction, which is essential for sperm-egg membrane fusion, involves a fusion-fission process between the plasma membrane and the outer acrosomal membrane, leading to the release of acrosomal contents (16, 17). The acrosome reaction in various species can be induced by physiological and nonphysiological substances, like progesterone and calcium ionophore 23187 (17, 18). Additionally, the acrosome reaction is regulated by different signal pathways including various phospholipases and lipid signaling molecules (17, 19, 20). Thus, capacitation and the acrosome reaction are continuous but different processes in mammalian sperm (17).

However, it remains elusive how the overall lipidomic characteristics of human spermatozoa change during capacitation and the acrosome reaction despite previous research documenting the involvement of specific lipid species in mammalian spermatozoa. This study aims to investigate lipidomic changes and differences between capacitation and the acrosome reaction in human spermatozoa using ultra-performance liquid chromatography-mass spectrometry (UPLC-MS) analysis and an untargeted strategy. Contrary to targeted studies focusing on quantifying specific compounds (21), the untargeted approach facilitates the analysis of all detectable metabolites—both known and unknown—thereby unveiling significant disparities between groups (22). Additionally, the present study utilized statistical methodologies such as unsupervised principal component analysis (PCA), supervised partial least-squares latent structure discriminate analysis (PLS-DA), and bidirectional orthogonal partial least squares (O2PLS) analysis. The result revealed the identification of twelve prominent differentiating lipids or metabolites between acrosome-reacted sperm induced by A23187 and uncapacitated as well as capacitated sperm in humans. These findings demonstrate the effectiveness of combining UPLC-MS-based lipidomics and multivariate analysis within an untargeted strategy to discern distinctive lipids across physiological states in sperm. Furthermore, they provide fresh insights into understanding lipid

physiology during the acrosome reaction and capacitation in human sperm.

Materials and methods

Chemical reagents

The human tubal fluid (HTF) medium was prepared using previously described methods (23, 24). The HTF medium (100 ml) comprised the following components: 90.0 mM NaCl, 25.05 mM $NaHCO_3$, 4.96 mM KCl, 6.98 mM $MgCl_2$, 1.80 mM $CaCl_2{\cdot}2H_2O$, 10.0 mM glucose, 10.0 mM sodium lactate, 0.27 mM sodium pyruvate, 1.17 mM KH_2PO_4, 2.0 mM HEPES, 400 mg BSA (fraction V, fatty acid-free), and 6 mg penicillin G. Sperm Wash® and gradient 40% and 80% (Sperm Filter®) were obtained from Cryos, Denmark. Calcium ionophore A23187 was sourced from Sigma Aldrich (Steinheim, Germany). Dimethyl sulfoxide (DMSO) was acquired from Merck (Darmstadt, Germany). Methanol was procured from Sigma-Aldrich (LC-MS CHROMASOLV®, ≥99.9%, Fluka®, Steinheim, Germany). Chloroform was supplied by Juhua Group Corporation (Zhejiang, China). Acetic acid was ordered from Sinopharm Chemical Reagent Co., Ltd (Shanghai, China). HPLC-grade formic acid was sourced from Sigma-Aldrich (St Louis, MO). Distilled water was purified with a Milli-Q system (Millipore, Bedford, MA).

Sperm preparation and study design

This study was reviewed and approved by the Medical Ethics Committee at the Zhejiang Academy of Medical Sciences. Semen samples were donated by the healthy men who provided written informed consent. The semen samples were obtained from individuals without any reproductive disorders. The experimental design is depicted in Figure 1. Samples were collected in sterile plastic containers through masturbation after a period of sexual abstinence lasting 3–5 days. Semen parameters were assessed following the guidelines of the World Health Organization (25). Semen samples containing other cell types were excluded from the study. Twelve semen samples meeting the criteria for normospermia were used. Sperm preparation was carried out as previously described (26). Briefly, sperm were separated from seminal plasma, via centrifugation using discontinuous Ready-to-use gradients of 40% and 80% (Sperm Filter®) at 800 x g for 15 min. The pellets were washed twice in centrifuge tubes with ten times the volume of Sperm Wash® by centrifugation at 300 g for 5 min. The concentrations were then adjusted to 2 x 10^6 cells/ml using HTF medium. The sperm suspension was divided into three groups before lipid extraction (1) the uncapacitated group, sperm were kept under noncapacitated conditions, on ice without 5% CO_2 incubation as human sperm do not undergo capacitation at temperatures below 37°C (27); (2) the capacitated group, sperm were incubated for capacitation at 37°C in 5% CO_2 for 5 h; (3) the acrosome reacted group, sperm were incubated for capacitation at 37°C in 5% CO_2 for5 h, and treated with 10 µM A23187 (final concentration) for 15 min.

Lipid extraction

Lipids were extracted from sperm under various conditions following the method described (28). Sperm were washed with PBS via centrifugation at 700 x g for 8 min. After resuspending the pellets in 400 µl PBS, they were vortexed in a mixture of 1.5 ml chloroform and methanol (1:2, v/v), and incubated at room temperature for 30 min. Subsequently, 0.5 ml chloroform was introduced into the mixture, followed by the addition of 0.5 ml acetic acid (40 mM), and then centrifuged at 1000 x g for 20 min. The lower chloroform phase was collected, and the remaining suspension underwent an additional extraction with 1 ml chloroform. The collected phases were combined into a single vial and dried using a nitrogen stream. The capped vials were stored at -80°C until lipid analysis.

Lipidomics profiles acquisition

The lipidomic characteristics of all extracted sperm were initially analyzed in the same batch using UPLC–MS based on the mass-to-charge ratio (m/z) and retention time (RT) (29). A reversed-phase analysis was performed using a Waters ACQUITY UPLC system (Waters Corporation, USA) equipped with an ACQUITY UPLC BEH C18 analytical column (particle size 1.7 µm, pore size 130 Å, dimensions 2.1 mm × 100 mm). Mobile phases A and B consisted of water/formic acid (99.9:0.1, v/v) and methanol/formic acid (99.9:0.1, v/v), respectively. The column was maintained at 50°C, and elution followed a gradient over 25 min: 0-0.5 min with 60% mobile phase B, 0.5-4 min increased to 80% B, 4-10 min increased to 98% B and held for 7 min, 17-18 min increased to 100% B and held for 1 min, 19-19.5 min mobile phase B was decreased to 3% and held for another 5.5 min for column re-equilibration. The flow rate was set at 0.3 ml/min, and the sample manager temperature was set at 4°C, with 2 µl of the sample injected into the column. Mass spectrometry was performed using the positive ion electrospray mode of the Waters Q-TOF Premier mass spectrometer (Waters Corporation, USA). Instrumental parameters were optimized as follows: a mass scan range of 50 to 1000 m/z with an accumulation time of 0.2 s per spectrum, an MS acquisition rate of 0.3 s, an interscan delay of 0.02 s, nebulizer and drying gas consisting of high-purity nitrogen, a nitrogen drying gas flow rate of 450 l/h, and a source temperature of 110°C. In the positive ion mode, the capillary voltage was set to 3.0 kV, the sampling cone voltage to 45.0 V, and the collision gas to Argon. MS/MS analysis was carried out with a varying collision energy of 10–50 eV, depending on the stability of each substance. The time-of-flight analyzer was used in V mode and tuned for maximum resolution (>10,000 resolving power at m/z 556.2771).

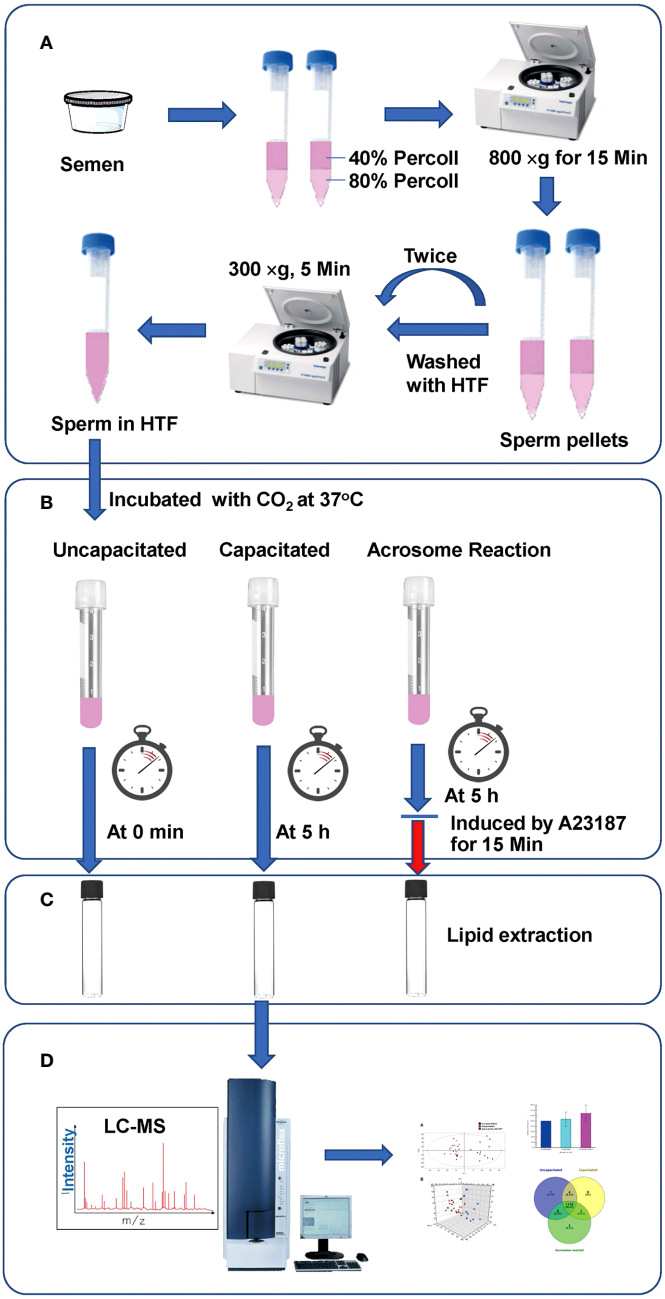

FIGURE 1
Workflow of our LC-MS-based lipidomics analysis. **(A)** Sperm Preparation; **(B)** Treatment of sperm under various conditions; **(C)** Lipid extraction; **(D)** Analysis via UPLC-MS.

The instrument was calibrated with sodium formate, and the lock mass spray for precise mass determination was set at 0.5 μg/ml leucine enkephalin at m/z 556.2771 in the positive ion mode. The quality control (QC) strategy is followed: QC samples were analyzed at intervals of eight samples during the analytical run, and the accuracy and precision of the assay method were evaluated via the QC sample analysis. All analyses were acquired via the lock spray to ensure accuracy and reproducibility, with the lock spray frequency set at 5 s, and data averaged over ten scans. Data were collected in centroid mode.

Data processing and analysis

All data from UPLC–MS analyses underwent processing using MarkerLynx applications with Waters MassLynx software (v4.1, Waters). Lipids were identified and validated using the Progenesis QI software. Peak intensities of the samples were detected, integrated, and normalized with applications (29–33). The primary parameters were applied according to the supporting information provided by the software. The total peak area for each sample was defined as a constant of 1000. To investigate the

differences between the groups, the lipidomic features were statistically analyzed using multivariate data analysis.

The resulting multivariate datasets comprised a single matrix with RT–m/z pairs for each file and were analyzed with SIMCA-P$^+$ 14.0 (Umetrics AB, Sweden) using multivariate data analysis techniques to visualize lipid clustering among different groups of samples. Before statistical analysis, data were normalized, mean-centered, and Pareto-scaled (29–31). An initial unsupervised PCA was used for general clustering visualization and outlying detection. Subsequently, supervised PLS-DA and bidirectional orthogonal partial least squares (O2PLS) analysis were performed to identify lipidomic changes between different conditions contributing to the observed clustering in the PCA (29–31, 34). To prevent model overfitting, the supervised models were validated with a permutation test repeated 200 times. Lipids potentially changed between different groups were selected based on variable importance in the projection (VIP) values and the S-plot. VIP values reflect the influence of each lipid composition on group differences while the S-plot, a loading plot, visually assisted in selecting major altered lipids. Variables farthest from the origin in S-plots significantly contribute to the inter-group differences (29).

Statistical analysis

The statistical significance of the data in different treatment groups was analyzed using SPSS 25.0 software. The one-way ANOVA test and the Mann-Whitney test were employed to evaluate the statistical significance between different groups ($P < 0.05$). Before analysis, normal distribution using the Shapiro-Wilk test and homogeneity of variances in the data among different groups was assessed. To identify potential lipids with differences between groups, the databases of CEU Mass Mediator (http://ceumass.eps.uspceu.es/mediator), LIPID MAPS (https://www.lipidmaps.org/), and HMDB (https://www.hmdb.ca/) were queried with the exact mass of lipids (and retention time). Additionally, Progenesis QI software (Waters) was used to validate the MS/MS profiles of the identified lipids.

Results

Lipidomics profiling of UPLC-MS in sperm under uncapacitated, capacitated, and acrosome-reacted conditions

To delineate lipid alterations, we processed thirty-six sperm samples from twelve subjects following the experimental workflow outlined in Figure 1. Figure 2 displays the base peak chromatograms of sperm in uncapacitated, capacitated, and acrosome-reacted states The lipidomic peaks observed in the three conditions were similar, indicating stable detection conditions and consistent major lipid species, such as 2.92_274.2748, 7.67_304.2596, and 12.08_792.5936. However, specific base peaks exhibited differences in intensity and presence among the different physiological conditions. For example, the base peak at 4.76_524 was absent in the uncapacitated and capacitated sperm but present in the acrosome-reacted group. Additionally, the base peak at 6.26_507.3298 exhibited higher intensity in the capacitated group compared to the uncapacitated and acrosome-reacted groups. The relative intensity of this base peak was lower in uncapacitated and capacitated sperm in comparison to acrosome-reacted sperm. These findings suggest that lipidomic profiles fluctuate based on different conditions, which can be detected through UPLC-MS analysis.

Disparities in the count of lipid peaks among individuals were observed when analyzing sperm under uncapacitated, capacitated, and acrosome-reacted states (Figure 3). The Venn diagram illustrates the overlap of 1176 lipid peaks across the twelve

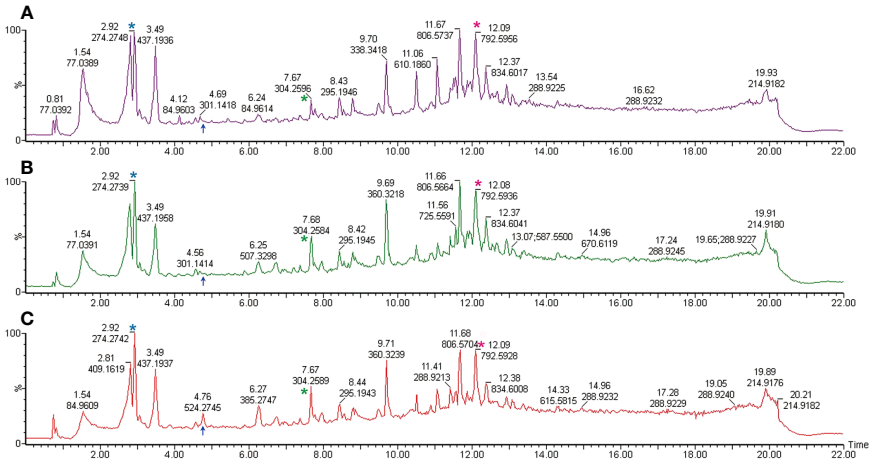

FIGURE 2
Representative total ion current chromatogram obtained from UPLC-MS. Samples are derived from the spermatozoa of one individual under differing conditions. **(A)** Uncapacitated sperm; **(B)** Capacitated sperm; **(C)** Acrosome-reacted sperm (induced by A23187). The illustration corresponds to one representative sample from each of the twelve experimental samples. The X-axis denotes the retention time, while the Y-axis represents the relative peak intensity. Common peaks are indicated with asterisks in the same colors, while different peaks are marked with blue arrows.

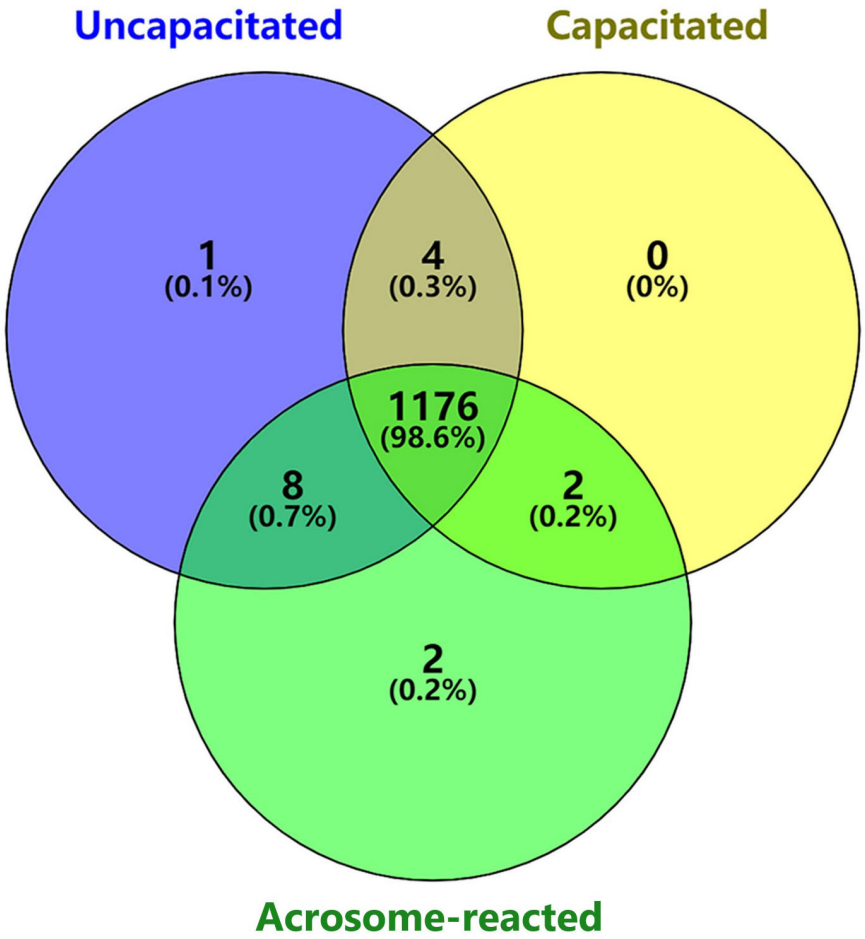

FIGURE 3
Venn diagram illustrating the number of unique and shared lipids identified among different sperm physiological states. Purple represents uncapacitated; Yellow, capacitated; Green, acrosome-reacted (A23187-induced).

individuals in the uncapacitated, capacitated, and acrosome-reacted groups. Furthermore, 1180 peaks overlapped between the uncapacitated and capacitated groups, 1184 peaks between the uncapacitated and acrosome-reacted groups, and 1178 peaks between the capacitated and acrosome-reacted groups. It is noteworthy that the count of overlapping peaks varied among individuals, ranging from 739 to 963 across sperm samples in the conditions (Refer to Supplementary Figure 1). Moreover, there were several peaks unique to specific groups. These results indicate that the lipid composition in sperm is influenced by different states and exhibits inter-individual variability. Untargeted studies can provide valuable information about global lipid profiles in individuals.

Acquisition and validation of UPLC-MS data through multivariate analysis models

To identify lipids or metabolites, we analyzed 1193 peaks in sperm under three different treatment conditions, uncapacitated, capacitated, and acrosome-reacted, using UPLC-MS. To simplify data interpretation without bias, we employed unsupervised statistical analysis, specifically PCA for the three groups. The PCA yielded five principal components (PCs), and the scatter score plot comparing PC1 and PC2 did not reveal any outliers among the uncapacitated, capacitated, and acrosome-reacted groups (Figure 4B). The PCA model explained 63.2% of the variance (R^2X) and predicted 40.5% (Q^2) of the variance based on cross-validation (Figure 4A).

For further class differentiation, supervised PLS-DA score plots were generated for the thirty-six samples. The results showed a clear separation between the uncapacitated and capacitated groups (Figure 5A), the uncapacitated group and the A23187-induced acrosome-reacted group (Figure 5B), and the capacitated group and the acrosome-reacted group (Figure 5C). Notably, no significant difference was observed between the uncapacitated and capacitated groups (Figure 5D). Subsequently, we developed an orthogonal partial least squares discriminant analysis (O2PLS-DA) model (1 + 5 + 0) to amplify the separation between the uncapacitated and capacitated groups as well as the A23187-induced acrosome-reacted group. The O2PLS-DA model (1 + 5 + 0) exhibited clear separation among the uncapacitated, capacitated, and acrosome-reacted groups (Figure 6A) with

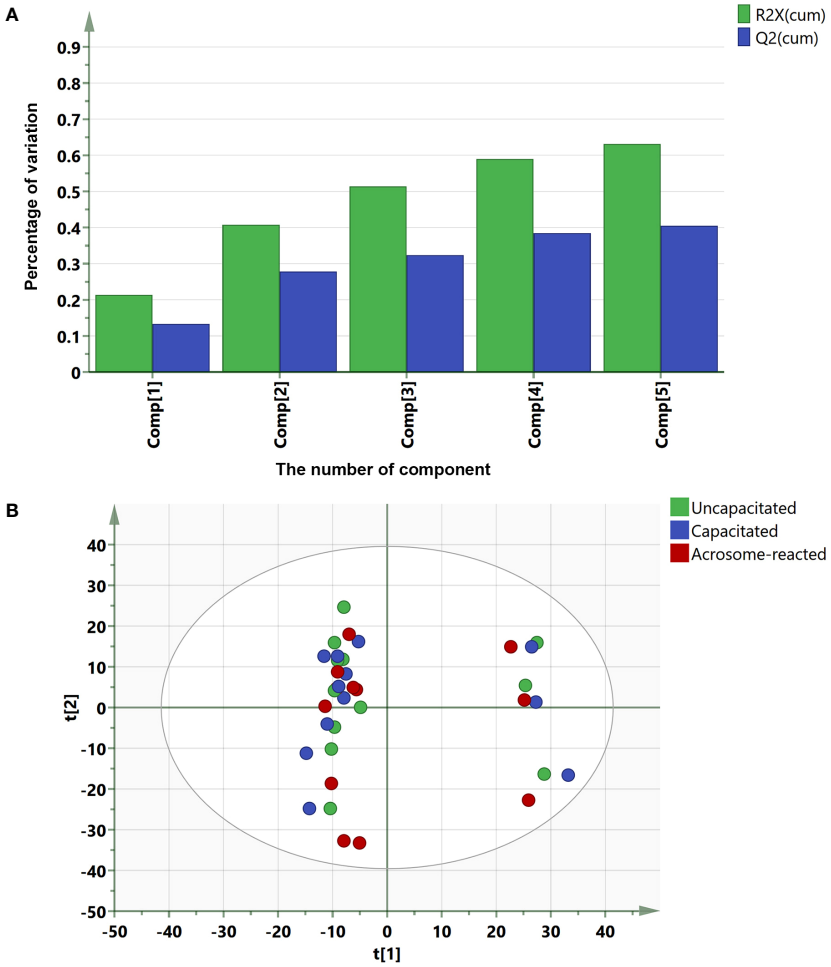

FIGURE 4
Summary of PCA fit and scores plot based on UPLC-MS data. **(A)** PCA fit summary; **(B)** Corresponding scores plot. Different circles represent different samples from twelve individuals. Blue, uncapacitated; Green, capacitated; Red, Acrosome-reacted.

validated modeling (R^2X, 65.3%; R^2Y, 46.4%; and Q^2, 0.155). The Distance to Model in the X space (DModX) plot of the O2PLS-DA model indicated that observations had values below 2.0, signifying their classification as standard observations in terms of variable correlation structure (Figure 6B). The predictive ability of the O2PLS-DA model was validated using a permutation test, which confirmed that the model did not overfit and outperformed 200 different permuted models (intercept of R^2: 0.33; intercept of Q^2: -0.292) (Figure 6C). The scatter plot of Y predictions showed a regression line with an R^2 value of 0.9066, indicating a good model fit (Figure 6D).

Identification of distinct lipids between acrosome-reacted group and uncapacitated/capacitated group

To identify the lipids contributing to group differentiation and elect significant candidate variables, we initially evaluated the VIP scores of variables (per the rationale: VIP-values >1 indicate importance; < 0.5, unimportance; and the range between 1 and 0.5, uncertainty in the importance, depending on the data set size) (Figure 7) and identified significant regions in the S-plot of the O2PLS-DA model (Figure 8). Based on VIP scores exceeding 1.5 and statistical significance, we selected and identified the top twelve candidate variables, which are categorized and presented in Table 1. These candidate variables included diacylglycerophosphoinositols (PI), monoacylglycerophosphoserines (LPS), monoacylglycerophosphates (LPA), oxidized glycerophosphoethanolamines (LPE), fatty acyls (FA), glycerophosphocholines (PC), glycerophosphoserines (PS), glycerophosphates (PA), and ceramide phosphocholines (SM, sphingomyelins). These findings suggest that these lipid metabolites play roles in biological functions during the acrosome reaction in human sperm.

Discussion

To the best of our knowledge, this study has been the first time to investigate the lipid profiles associated with acrosome reaction and capacitation in human sperm, utilizing UPLC-MS in

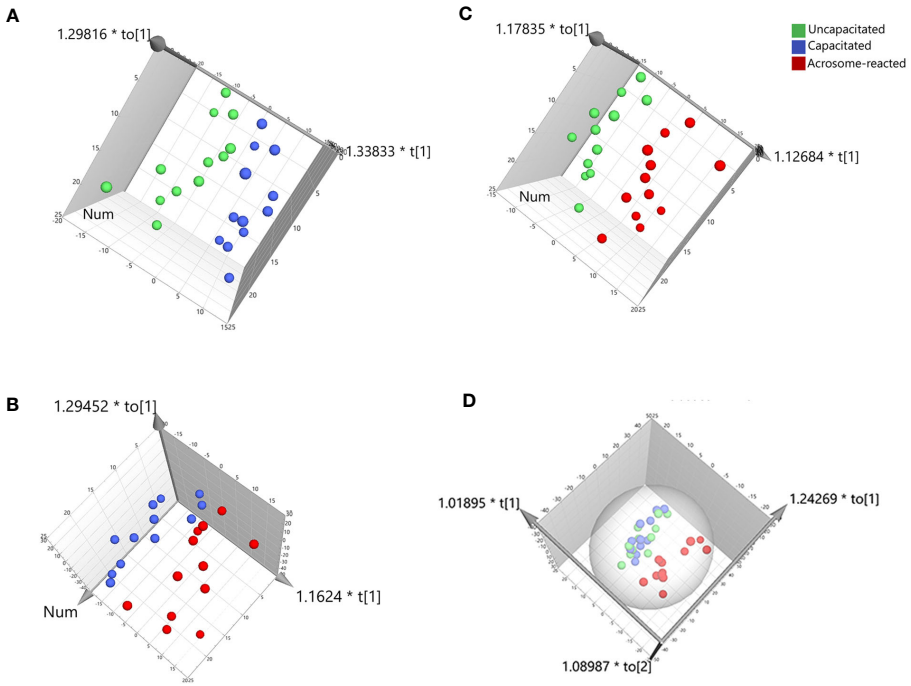

FIGURE 5
PLS-DA score plot derived from UPLC-MS data in the positive ion mode. **(A)** Comparison between Uncapacitated and Capacitated states; **(B)** Comparison between Uncapacitated and A23187-induced Acrosome-reacted states; **(C)** Comparison between Capacitated and Acrosome-reacted states; **(D)** Consolidated plot of **(A–C)**.

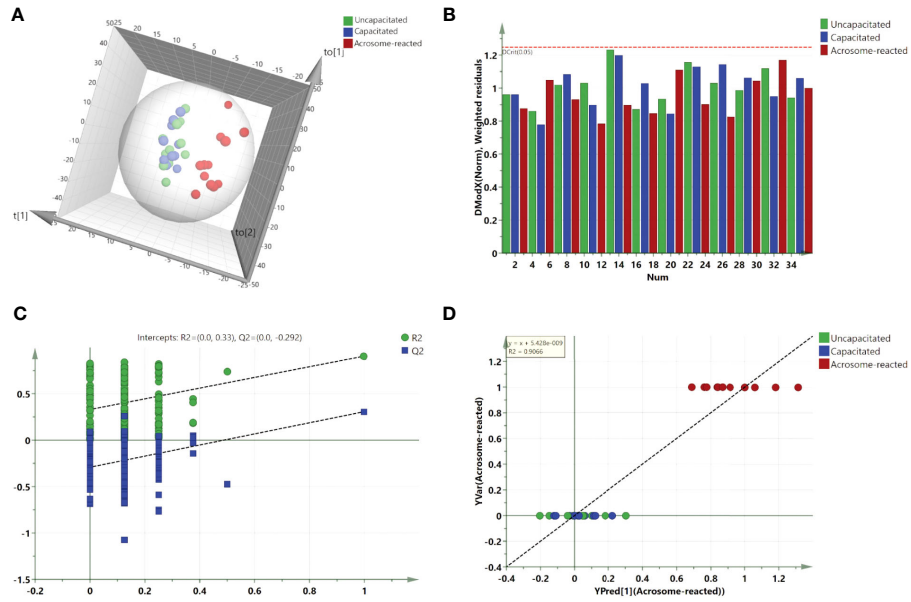

FIGURE 6
Validation and O2PLS-DA scores plot derived from UPLC-MS data in the positive ion mode. **(A)** O2PLS-DA scores plot comparing Uncapacitated and Capacitated states with Acrosome-reacted samples; **(B)** DModX plot of the O2PLS-DA model, demonstrating that the observations fall within the normal range when considering the correlation structure of the variables; **(C)** Validation plot of the combined model, based on 200 permutation tests. The R^2 value (green line) signifies explained variance, and the Q^2 value (blue line) denotes the predictive ability of the model. Lower calculated R^2 and Q^2 values than the original, and a Q^2 intersecting the vertical axis below zero, confirm the model's validity. **(D)** Y prediction scatter plot of all sperm samples as per the O2PLS-DA model.

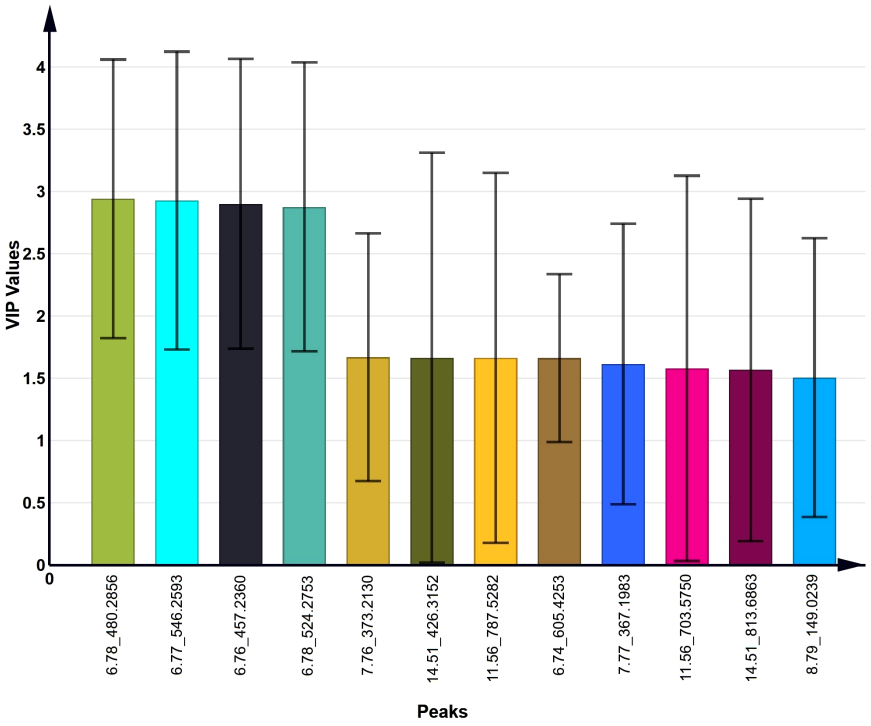

FIGURE 7
The top 12 VIP values of candidate variables obtained from the O2PLS-DA model.

conjunction with multivariate data analysis. It provides an in-depth analysis of metabolic lipids under various physiological states, encompassing the assessment of 1193 distinct lipids during uncapacitated, capacitated, and A23187-induced acrosome reaction states. It is noteworthy that the counts of lipid exhibited variability among individuals under different conditions (Refer to Supplementary Figure 1). This variability in the lipid metabolic compositions among individuals can be attributed to genetics and epigenetic variations influencing the expression and activity of enzymes and proteins involved in lipid metabolism as well as factors related to health conditions, lifestyle choices, and environmental exposures affecting lipid metabolism.

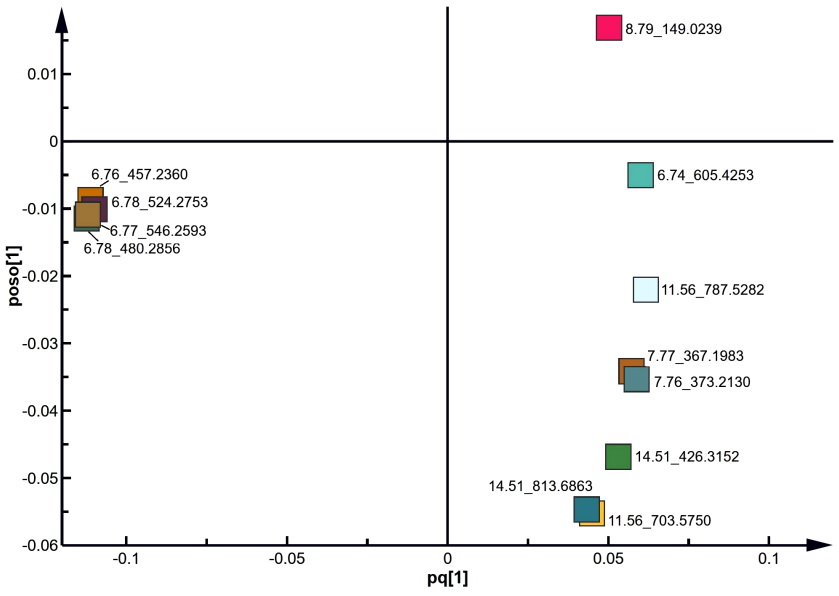

FIGURE 8
S plot derived from the O2PLS-DA model using UPLC-MS data.

TABLE 1 The predominant discrimination metabolites in human sperm under the different physiological status.

No.	Rt_M/Z	Adducts	Identified Results	Common Name	Systematic Name	Uncapacitated	Capacitated	Acrosome-Reacted
1	6.78_480.2856	$[M+2H]^+$	PI 44:10	PI (22:4 (7Z,10Z,13Z,16Z)/22:6 (4Z,7Z,10Z,13Z,16Z,19Z))	1-(7Z,10Z,13Z,16Z-docosatetraenoyl)-2-(4Z,7Z,10Z,13Z,16Z,19Z-docosahexaenoyl)-glycero-3-phospho-(1'-myo-inositol)	0.01 ± 0.04	0.03 ± 0.07	5.39 ± 3.89^{ac,bc}
2	6.77_546.2593	$[M+H]^+$	LPS 20:4	PS (20:4 (5Z,8Z,11Z,14Z)/0:0)	1-(5Z,8Z,11Z,14Z-eicosatetraenoyl)-sn-glycero-3-phosphoserine	0.01 ± 0.02	0.05 ± 0.13	22.29 ± 16.51 $^{ac, bc}$
3	6.76_457.2360	$[M+H]^+$	LPA 20:5	LysoPA (20:5 (5Z,8Z,11Z,14Z,17Z) /0:0)	1-(5Z,8Z,11Z,14Z,17Z-eicosapentaenoyl)-glycero-3-phosphate	0.00 ± 0.00	0.00 ± 0.00	2.14 ± 1.65 $^{ac, bc}$
4	6.78_524.2753	$[M+Na]^+$	LPE 20:4	LysoPE (0:0/20:4 (8Z,11Z,14Z,17Z))	2-(8Z,11Z,14Z,17Z-eicosatetraenoyl)-sn-glycero-3-phosphoethanolamine	0.26 ± 0.26	0.49 ± 1.00	113.17 ± 87.42 $^{ac, bc}$
5	7.76_373.2130	$[M+H]^+$	FA 22:8;O3	16-phenyl-tetranor-PGE2	9-oxo-11R,15S-dihydroxy-16-phenyl-17,18,19,20-tetranor-5Z,13E-prostadienoic acid	1.38 ± 0.75	1.01 ± 0.53	0.60 ± 0.37 ^{ac}
6	14.51_426.3152	$[M+H+NH_4]^+$	PC 40:6	PC (18:0/22:6 (9Z,11Z,13Z,15Z,17Z,19))	1-octadecanoyl-2-(9Z,11Z,13Z,15Z,17Z,19-docosahexaenoyl)-sn-glycero-3-phosphocholine	6.52 ± 1.51	6.34 ± 1.50	5.19 ± 1.84^{bd}
7	11.56_787.5282	$[M+NH_4]^+$	PS 35:4	PS (22:4 (7Z,10Z,13Z,16Z)/13:0)	1-(7Z,10Z,13Z,16Z-docosatetraenoyl)-2-tridecanoyl-glycero-3-phosphoserine	10.63 ± 3.50	11.15 ± 2.88	7.90 ± 2.74^{bd}
8	6.74_605.4253	$[M+H]^+$	PA 29:1	PA (12:0/17:1(9Z))	1-dodecanoyl-2-(9Z-heptadecenoyl)-glycero-3-phosphate	4.19 ± 1.65	4.06 ± 0.96	3.08 ± 1.00 ^{ad}
9	7.77_367.1983	$[M+NH_4]^+$	FA 20:5;O4	20-carboxy-LTB4	5S,12R-dihydroxy-6Z,8E,10E,14Z-eicosatetraene-1,20-dioic acid	3.63 ± 1.62	2.38 ± 1.56^{ad}	1.50 ± 0.94 ^{ac}
10	11.56_703.5750	$[M+H]^+$	SM 34:1;O2	SM (d16:1/18:0)	N-(octadecanoyl)-hexadecasphing-4-enine-1-phosphocholine (Ceramide phosphocholines (sphingomyelins)	50.12 ± 10.66	49.24 ± 11.64	42.22 ± 14.05
11	14.51_813.6863	$[M+H]^+$	SM 42:2;O2	SM (d18:1/24:1(15Z))	N-(15Z-tetracosenoyl)-sphing-4-enine-1-phosphocholine	18.08 ± 4.73	16.82 ± 4.46	14.61 ± 5.45
12	8.79_149.0239	$[M+H]^+$	FA	2-oxo-4-methylthio-butanoic acid	2-oxo-4-methylthio-butanoic acid	10.96 ± 2.03	11.79 ± 2.64	9.48 ± 2.25^{bd}

All data are presented as mean ± SD of peak intensities. The statistical significance was analyzed using SPSS 25.0 software. The one-way ANOVA test and the Mann-Whitney test were performed. Before analysis, normal distribution using the Shapiro-Wilk test and homogeneity of variances in the data among different groups was assessed. P values < 0.05 were considered statistically significant. a denotes comparison with the uncapacitated group, b denotes comparison with the capacitated group, c indicates P < 0.01, and d indicates P < 0.05. Lipids are formally identified by standard samples or published data. lipids putatively annotated by library searching.

RT, retention time; m/z, mass-to-charge ratio; VIP, variable importance in the project values; PI, diacylglycerophosphoinositols; LPS, monoacylglycerophosphoserines; LPA, monoacylglycerophosphates; LPE, oxidized glycerophosphoethanolamines; FA, fatty acyls; PC, glycerophosphocholines; PS, glycerophosphoserines; PA, glycerophosphates; SM, ceramide phosphocholines (sphingomyelins).

10.3389/fendo.2023.1273878

Furthermore, based on the VIP list derived from the O2PLS-DA model, 137 lipids had VIP values exceeding 1.0, and twenty-two lipids had VIP values exceeding 1.5. Among the identified lipids, twelve metabolites were categorized into three groups (Table 1): four lipids exhibited increased levels, six lipids showed decreased levels, and two lipids did not show statistically significant changes. These findings underscore the significant divergence in lipid composition during the A23187-induced acrosome reaction compared to uncapacitated and capacitated states in human sperm.

This study unveiled a higher level of PI 44:10 during the A23187-induced acrosome reaction (Table 1). The observed increase in PI within human sperm aligns with findings from a prior study employing a different analytical method (35). Additionally, the increased PI induced by A23187 aligns with reports in the platelet system (36). Polyphosphoinositides (PPIn) are critical signaling phospholipids that play a significant role in the composition of cellular membranes and signaling cascades in mammalian cells (37) and sperm development (38). The metabolism of polyphosphoinositides is closely linked to the activity of phosphatase and tensin homolog (PTEN) identified in human sperm during the acrosome reaction (39). This signaling pathway suggests a close association between the acrosome reaction and lipid phosphatases that remove phosphate groups through dephosphorylate, such as PTEN, SYNJ1, and SYNJ2 (37).

A significantly lower level of phosphatidylcholine (PC) 40:6 was observed during induction by A23187. These results align with previous research demonstrating a reduction in PC during acrosome reaction (40). The decline of PC levels in acrosome-reacted sperm may be a result of hydrolysis by phospholipase C (41) or phospholipase A2 (PLA_2) (42), leading to the production of LysoPC. LysoPC, a byproduct of PC hydrolysis, independently modulates ionic gradients and induces depolarization of the sperm membrane (43), thereby enhancing sperm penetration rate and acrosome reaction (44). Additionally, it modifies the zona pellucida and the plasma membrane of both gametes *in vitro*, promoting gamete fusion (45). LysoPC is closely associated with sperm motility (46–48), the freeze/thaw cycle of sperm (49), obesity (50), and male infertility (51). LysoPC is often used as an inducer of the acrosome reaction (52) to treat spermatozoa in cases of male infertility because it increases fertilization rates in IVF (44). PC metabolism through the production of LysoPC is crucial for sperm function and fertilization.

Two classes of sphingomyelin (SM), a sphingolipid variant found in sperm plasma membranes, exhibited changes in human sperm subjected to A23187 induction, in comparison to uncapacitated and capacitated sperm. SM encompasses various molecular species, including relatively long saturated chains (16:0, 18:0, and 24:0), very long-chain polyunsaturated fatty acids (ranging from 24:0 to 34:0), and elongated versions of common PUFA from the n-6 or n-3 series (53). Our findings align with decreasing trends observed in a similar context in a previous investigation (54), although statistical significance was not observed in the present study. Furthermore, SM in mammalian sperm often contains very long-chain polyunsaturated fatty acids and can accelerate the acrosome reaction stimulated by progesterone, linked to PLA_2 activity during the acrosome reaction (55).

Modifications in other phospholipids were observed in sperm subjected to A23187-induced acrosome reaction, as compared to capacitated and uncapacitated sperm. Specifically, LPS 20:4, LPA 20:5, and LPE 20:4 showed an increase, while PS 35:4 and PA 29:1 showed a decrease. The synthesis of PS, PA, and PC relates to glycerol-3-phosphate, known as the Kennedy pathway. Lipids such as LPA 20:5 may be regulated by glycerol-3-phosphate acyltransferases (GPATs), which esterify an acyl chain of glycerol-3-phosphate (G3P) to G3P at the sn-1 position, and LPA-acyltransferases (LPAATs), which esterify a second acyl chain of LPA to the sn-2 position to produce PA. The observed increase in PA in this study is consistent with a prior study (35). PA can be dephosphorylated by PA phosphatases (PAPs) to produce the lipid second messenger diacylglycerol (DAG), which can further be metabolized to produce PC, PE, PS, and triglyceride (TG). LPS, PS, and LPE change in the Lands' cycle reaction and are associated with specific enzymes like LPEAT, LPSAT, LPIAT, and PLA_2. On the other hand, PA may be acted upon by cytidine diphosphate (CDP)-DAG synthase to produce CDP-DAG, which can be further metabolized to produce PI (56) and affect the PI pathway. In this process, phospholipases, including the main PLA_2 and phospholipases C (PLC), play roles in regulating lipid metabolism and lipid signaling molecules, participating in various signal pathways: PLA_2 action on PC, PE, or PI generates lysoPC, lysoPE, or lysoPI as well as fatty acids such as arachidonic, oleic, linoleic, linolenic, or docosahexaenoic acid; phosphoinositide-specific PLC (PPI-PLC) mediated hydrolysis of phosphatidylinositol 4,5-bisphosphate generates 1,4,5-trisphosphate (IP3) and DAG; and PC-PLC hydrolysis of phosphatidylcholine yields choline phosphate and DAG (19, 20).

Furthermore, observations also indicated metabolic variations in different fatty acids, such as FA 22:8-O3 and FA 20:5-O4, during the A23187-induced acrosome reaction. FA 22:8-O3, also known as 16-phenyl-tetranor-prostaglandin E2 (PGE2), has been reported as a stable derivative of PGE2 that acts on its receptor (57). This result is consistent with previous studies indicating that prostaglandins play an important role in the sperm acrosome reaction (58). The other fatty acid, FA 20:5-O4, also known as 20-carboxy-leukotriene B4 (LTB4), has been associated with the action of calcium ionophores (59). LTB4 is biosynthesized from arachidonic acid released from membrane phospholipids through the activity of cytosolic and various types of PLA_2s (60). LTB4 can induce the acrosome reaction when present throughout the preincubation period, suggesting that it may enhance the capacitation process rather than the acrosome reaction. Additionally, LTB4 is one of the metabolites linked to the adverse effects of environmental arsenic exposure on humans (61).

Of utmost importance, this study is the first to detect 2-oxo-4-methylthiobutanoic acid (OMBA), during the A23187-induced

acrosome reaction. OMBA falls within the category of fatty acids and conjugates of lipids, as per lipidmaps.org, and serves as an intermediate in the metabolism of cysteine and methionine. OMBA has previously been associated with male infertility and arsenic exposure (61) and has been discussed as a metabolite marker in recent studies (62–64). It is proposed that OMBA's impact on sperm viability may be mediated through methionine oxidation (65). Additionally, OMBA participates in the seven signaling pathways, according to the Kyoto Encyclopedia of Genes and Genomes (KEGG) Pathway Database, including cysteine and methionine metabolism, amino acid metabolism, glucosinolate biosynthesis, biosynthesis of plant secondary metabolites, metabolic pathways, biosynthesis of secondary metabolites, and oxo-carboxylic acid metabolism. The involvement of OMBA in diverse signaling pathways suggests its potential significance in sperm physiology. In all, this study suggests that OMBA and its associated signaling pathways may play a crucial role in the acrosome reaction, with further mechanistic investigations warranted in the future.

Furthermore, the applications of UPLC-MS in conjunction with multivariate data analysis effectively highlighted the dominant lipids involved in the A23187-induced acrosome reaction in human sperm. The untargeted lipidomics strategy provided comprehensive insights into the lipid composition of sperm in different physiological conditions, allowing for the detection, analysis, and differentiation of major compounds without bias. Compared to targeted strategies with specific aims, the untargeted strategy harnessed the full m/z information of molecular structure using UPLC-MS, surpassing previous lipid studies that employed various chromatography techniques. This study underscores the value of the untargeted lipidomics strategy for studying lipid metabolism and characterizing physiological states in sperm.

While acknowledging the significance, this study's limitations should be recognized. The lipidomics analysis was exclusively performed with the positive model of UPLC-MS, potentially leading to the non-detection of some compounds in the neutral and negative ion model, thus bypassing the partial metabolites and signaling pathways. Additionally, the sample size of twelve individuals may be limited although this study has already yielded valuable insights into these differences in different physiological states. Therefore, future investigations, involving larger sample sizes and more diverse cohorts, may be necessary to thoroughly elucidate differences in lipid composition, validate findings, and generalize the results.

Conclusions

This study has shed light on the variations in lipid composition among uncapacitated, capacitated, and acrosome-reacted sperm. Twelve significant lipids or metabolites were discerned between A23187-induced acrosome-reacted sperm and the uncapacitated/capacitated sperm in humans. The results corroborate earlier discoveries on lipids during the acrosome reaction and unveil a new metabolite OMBA. This investigation demonstrates the effectiveness of an untargeted approach using UPLC-MS-based lipidomics and multivariate analysis for identifying discriminating lipids in different physiological stages of sperm. Additionally, it provides novel insights into lipid metabolism during capacitation and the acrosome reaction in human sperm, which holds significance in the context of male reproduction.

Data availability statement

The data presented in the study are deposited in the figshare repository, and can be found here https://doi.org/10.6084/m9.figshare.24223207.v2.

Ethics statement

The studies involving humans were approved by the Medical Ethics Committee at the Zhejiang Academy of Medical Sciences. The studies were conducted in accordance with the local legislation and institutional requirements. The participants provided their written informed consent to participate in this study.

Author contributions

XC: Conceptualization, Investigation, Writing – original draft. HX: Conceptualization, Investigation, Writing – review & editing. YuX: Investigation, Writing – review & editing. PS: Resources, Writing – review & editing. YaX: Conceptualization, Resources, Writing – review & editing. KL: Conceptualization, Data curation, Formal Analysis, Funding acquisition, Investigation, Methodology, Project administration, Resources, Software, Supervision, Validation, Visualization, Writing – original draft, Writing – review & editing.

Funding

The author(s) declare financial support was received for the research, authorship, and/or publication of this article. This work was supported by the Natural Science Foundation of China (No 81000244), Zhejiang Provincial Natural Science Foundation (LY22H040011), and Zhejiang Provincial Program for the Cultivation of High-Level Innovative Health Talents (Year 2018).

Acknowledgments

The authors thank the volunteers who donor the semen in this study.

Conflict of interest

The authors declare that the research was conducted in the absence of any commercial or financial relationships that could be construed as a potential conflict of interest.

Publisher's note

All claims expressed in this article are solely those of the authors and do not necessarily represent those of their affiliated organizations, or those of the publisher, the editors and the reviewers. Any product that may be evaluated in this article, or claim that may be made by its manufacturer, is not guaranteed or endorsed by the publisher.

Supplementary material

The Supplementary Material for this article can be found online at: https://www.frontiersin.org/articles/10.3389/fendo.2023.1273878/full#supplementary-material

References

1. Wenk MR. The emerging field of lipidomics. *Nat Rev Drug Discov* (2005) 4 (7):594–610. doi: 10.1038/nrd1776

2. Petcoff DW, Holland WL, Stith BJ. Lipid levels in sperm, eggs, and during fertilization in Xenopus laevis. *J Lipid Res* (2008) 49(11):2365–78. doi: 10.1194/jlr.M800159-JLR200

3. Basu S, Whiteman M, Mattey DL, Halliwell B. Raised levels of F(2)-isoprostanes and prostaglandin F(2alpha) in different rheumatic diseases. *Ann Rheum Dis* (2001) 60 (6):627–31. doi: 10.1136/ard.60.6.627

4. Graessler J, Schwudke D, Schwarz PE, Herzog R, Shevchenko A, Bornstein SR. Top-down lipidomics reveals ether lipid deficiency in blood plasma of hypertensive patients. *PLoS One* (2009) 4(7):e6261. doi: 10.1371/journal.pone.0006261

5. Han X. The emerging role of lipidomics in prediction of diseases. *Nat Rev Endocrinol* (2022) 18(6):335–6. doi: 10.1038/s41574-022-00672-9

6. Oresic M, Hanninen VA, Vidal-Puig A. Lipidomics: a new window to biomedical frontiers. *Trends Biotechnol* (2008) 26(12):647–52. doi: 10.1016/j.tibtech.2008.09.001

7. Shevchenko A, Simons K. Lipidomics: coming to grips with lipid diversity. *Nat Rev Mol Cell Biol* (2010) 11(8):593–8. doi: 10.1038/nrm2934

8. Zalata AA, Christophe AB, Depuydt CE, Schoonjans F, Comhaire FH. The fatty acid composition of phospholipids of spermatozoa from infertile patients. *Mol Hum Reprod* (1998) 4(2):111–8. doi: 10.1093/molehr/4.2.111

9. Shan S, Xu F, Hirschfeld M, Brenig B. Sperm lipid markers of male fertility in mammals. *Int J Mol Sci* (2021) 22(16):8767. doi: 10.3390/ijms22168767

10. Schiller J, Suss R, Fuchs B, Muller M, Zschornig O, Arnold K. MALDI-TOF MS in lipidomics. *Front Biosci J virtual library* (2007) 12:2568–79. doi: 10.2741/2255

11. Chen S, Wang M, Li L, Wang J, Ma X, Zhang H, et al. High-coverage targeted lipidomics revealed dramatic lipid compositional changes in asthenozoospermic spermatozoa and inverse correlation of ganglioside GM3 with sperm motility. *Reprod Biol Endocrinol RB&E* (2021) 19(1):105. doi: 10.1186/s12958-021-00792-3

12. Chang MC. Fertilizing capacity of spermatozoa deposited into the fallopian tubes. *Nature* (1951) 168(4277):697–8. doi: 10.1038/168697b0

13. Visconti PE. Understanding the molecular basis of sperm capacitation through kinase design. *Proc Natl Acad Sci USA* (2009) 106(3):667–8. doi: 10.1073/pnas.0811895106

14. Puga Molina LC, Luque GM, Balestrini PA, Marin-Briggiler CI, Romarowski A, Buffone MG. Molecular basis of human sperm capacitation. *Front Cell Dev Biol* (2018) 6:72. doi: 10.3389/fcell.2018.00072

15. Cohen-Dayag A, Eisenbach M. Potential assays for sperm capacitation in mammals. *Am J Physiol* (1994) 267(5 Pt 1):C1167–76. doi: 10.1152/ajpcell.1994.267.5.C1167

16. Hirohashi N, Yanagimachi R. Sperm acrosome reaction: its site and role in fertilization. *Biol Reprod* (2018) 99(1):127–33. doi: 10.1093/biolre/ioy045

17. Abou-haila A, Tulsiani DR. Signal transduction pathways that regulate sperm capacitation and the acrosome reaction. *Arch Biochem Biophys* (2009) 485(1):72–81. doi: 10.1016/j.abb.2009.02.003

18. Yanagimachi R. Mammalian fertilization. In: Knobil E, Neill JD, editors. *The Physiology of Reproduction*. New York: Raven Press (1994).

19. Li K, Shi QX, Ni Y. Signal transduction and regulation of phospholipase A2 during acrosomal exocytosis in spermatozoa. *Chin J Cell Biol* (2006) 28(03):410–4. doi: 10.3969/j.issn.1674-7666.2006.03.011

20. Roldan ER, Shi QX. Sperm phospholipases and acrosomal exocytosis. *Front Biosci J virtual library* (2007) 12:89–104. doi: 10.2741/2050

21. Gertsman I, Barshop BA. Promises and pitfalls of untargeted metabolomics. *J Inherit Metab Dis* (2018) 41(3):355–66. doi: 10.1007/s10545-017-0130-7

22. Want EJ, Cravatt BF, Siuzdak G. The expanding role of mass spectrometry in metabolite profiling and characterization. *Chembiochem* (2005) 6(11):1941–51. doi: 10.1002/cbic.200500151

23. Li K, Xue Y, Chen A, Jiang Y, Xie H, Shi Q, et al. Heat shock protein 90 has roles in intracellular calcium homeostasis, protein tyrosine phosphorylation regulation, and progesterone-responsive sperm function in human sperm. *PloS One* (2014) 9(12): e115841. doi: 10.1371/journal.pone.0115841

24. Li K, Ni Y, He Y, Chen WY, Lu JX, Cheng CY, et al. Inhibition of sperm capacitation and fertilizing capacity by adjudin is mediated by chloride and its channels in humans. *Hum Reprod* (2013) 28(1):47–59. doi: 10.1093/humrep/des384

25. World Health Organization. *WHO Laboratory Manual for the Examination and Processing of Human Semen*. Geneva: WHO Press (2010).

26. Li K, Sun P, Wang Y, Gao T, Zheng D, Liu A, et al. Hsp90 interacts with Cdc37, is phosphorylated by PKA/PKC, and regulates Src phosphorylation in human sperm capacitation. *Andrology* (2021) 9(1):185–95. doi: 10.1111/andr.12862

27. Marin-Briggiler CI, Tezon JG, Miranda PV, Vazquez-Levin MH. Effect of incubating human sperm at room temperature on capacitation-related events. *Fertil Steril* (2002) 77(2):252–9. doi: 10.1016/s0015-0282(01)02982-x

28. Lessig J, Gey C, Suss R, Schiller J, Glander HJ, Arnhold J. Analysis of the lipid composition of human and boar spermatozoa by MALDI-TOF mass spectrometry, thin layer chromatography and 31P NMR spectroscopy. *Comp Biochem Physiol Part B Biochem Mol Biol* (2004) 137(2):265–77. doi: 10.1016/j.cbpc.2003.12.001

29. Wang B, Chen D, Chen Y, Hu Z, Cao M, Xie Q, et al. Metabonomic profiles discriminate hepatocellular carcinoma from liver cirrhosis by ultraperformance liquid chromatography-mass spectrometry. *J Proteome Res* (2012) 11(2):1217–27. doi: 10.1021/pr2009252

30. Qiu Y, Cai G, Su M, Chen T, Liu Y, Xu Y, et al. Urinary metabonomic study on colorectal cancer. *J Proteome Res* (2010) 9(3):1627–34. doi: 10.1021/pr901081y

31. Coen M, Want EJ, Clayton TA, Rhode CM, Hong YS, Keun HC, et al. Mechanistic aspects and novel biomarkers of responder and non-responder phenotypes in galactosamine-induced hepatitis. *J Proteome Res* (2009) 8(11):5175–87. doi: 10.1021/pr9005266

32. Barr J, Vazquez-Chantada M, Alonso C, Perez-Cormenzana M, Mayo R, Galan A, et al. Liquid chromatography-mass spectrometry-based parallel metabolic profiling of human and mouse model serum reveals putative biomarkers associated with the progression of nonalcoholic fatty liver disease. *J Proteome Res* (2010) 9(9):4501–12. doi: 10.1021/pr1002593

33. Lin L, Huang Z, Gao Y, Yan X, Xing J, Hang W. LC-MS based serum metabonomic analysis for renal cell carcinoma diagnosis, staging, and biomarker discovery. *J Proteome Res* (2011) 10(3):1396–405. doi: 10.1021/pr101161u

34. Chen T, Xie G, Wang X, Fan J, Qiu Y, Zheng X, et al. Serum and urine metabolite profiling reveals potential biomarkers of human hepatocellular carcinoma. *Mol Cell Proteomics* (2011) 10(7):M110 004945. doi: 10.1074/mcp.M110.004945

35. Roldan ER, Harrison RA. Polyphosphoinositide breakdown and subsequent exocytosis in the Ca^{2+}/ionophore-induced acrosome reaction of mammalian spermatozoa. *Biochem J* (1989) 259(2):397–406. doi: 10.1042/bj2590397

36. Billah MM, Lapetina EG. Evidence for multiple metabolic pools of phosphatidylinositol in stimulated platelets. *J Biol Chem* (1982) 257(20):11856–9. doi: 10.1016/S0021-9258(18)33641-X

37. Dickson EJ. Recent advances in understanding phosphoinositide signaling in the nervous system. *F1000Res* (2019) 8 (F1000 Faculty Rev):278. doi: 10.12688/f1000research.16679.1

38. Brill JA, Yildirim S, Fabian L. Phosphoinositide signaling in sperm development. *Semin Cell Dev Biol* (2016) 59:2–9. doi: 10.1016/j.semcdb.2016.06.010

39. Koppers AJ, Mitchell LA, Wang P, Lin M, Aitken RJ. Phosphoinositide 3-kinase signalling pathway involvement in a truncated apoptotic cascade associated with motility loss and oxidative DNA damage in human spermatozoa. *Biochem J* (2011) 436(3):687–98. doi: 10.1042/BJ20110114

40. Lepage N, Roberts KD. Purification of lysophospholipase of human spermatozoa and its implication in the acrosome reaction. *Biol Reprod* (1995) 52(3):616–24. doi: 10.1095/biolreprod52.3.616

41. Roldan ER, Murase T. Polyphosphoinositide-derived diacylglycerol stimulates the hydrolysis of phosphatidylcholine by phospholipase C during exocytosis of the ram sperm acrosome. *Effect is not mediated by Protein kinase C J Biol Chem* (1994) 269 (38):23583–9. doi: 10.1016/S0021-9258(17)31555-7

42. Glander HJ, Schiller J, Suss R, Paasch U, Grunewald S, Arnhold J. Deterioration of spermatozoal plasma membrane is associated with an increase of sperm lyso-phosphatidylcholines. *Andrologia* (2002) 34(6):360–6. doi: 10.1046/j.1439-0272.2002.00508.x

43. Salazar EL, Macias H, Calzada L. [The role of hyperpolarization and depolarization of the membrane of the human spermatozoon]. *Ginecol Obstet Mex* (1991) 59:308–12.

44. Lachapelle MH, Bouzayen R, Langlais J, Jarvi K, Bourque J, Miron P. Effect of lysoplatelet-activating factor on human sperm fertilizing ability. *Fertil Steril* (1993) 59 (4):863–8. doi: 10.1016/S0015-0282(16)55873-7

45. Riffo M, Parraga M. Lysophosphatidylcholine treatment allows interspecies fertilization of hamster oocytes with zona pellucida by human spermatozoa. *J Exp Zool* (1995) 271(2):151–4. doi: 10.1002/jez.1402710211

46. Engel KM, Baumann S, Rolle-Kampczyk U, Schiller J, von Bergen M, Grunewald S. Metabolomic profiling reveals correlations between spermiogram parameters and the metabolites present in human spermatozoa and seminal plasma. *PloS One* (2019) 14(2): e0211679. doi: 10.1371/journal.pone.0211679

47. Hong CY, Shieh CC, Wu P, Huang JJ, Chiang BN. Effect of phosphatidylcholine, lysophosphatidylcholine, arachidonic acid and docosahexaenoic acid on the motility of human sperm. *Int J Androl* (1986) 9(2):118–22. doi: 10.1111/j.1365-2605.1986.tb00874.x

48. Jarvi K, Roberts KD, Langlais J, Gagnon C. Effect of platelet-activating factor, lyso-platelet-activating factor, and lysophosphatidylcholine on sperm motion: importance of albumin for motility stimulation. *Fertil Steril* (1993) 59(6):1266–75. doi: 10.1016/s0015-0282(16)55988-3

49. Schiller J, Arnhold J, Glander HJ, Arnold K. Lipid analysis of human spermatozoa and seminal plasma by MALDI-TOF mass spectrometry and NMR spectroscopy - effects of freezing and thawing. *Chem Phys Lipids* (2000) 106(2):145–56. doi: 10.1016/s0009-3084(00)00148-1

50. Pyttel S, Zschornig K, Nimptsch A, Paasch U, Schiller J. Enhanced lysophosphatidylcholine and sphingomyelin contents are characteristic of spermatozoa from obese men-A MALDI mass spectrometric study. *Chem Phys Lipids* (2012) 165(8):861–5. doi: 10.1016/j.chemphyslip.2012.11.001

51. Hula NM, Tron'ko MD, Volkov HL, Marhitych VM. [Lipid composition and fertility of human ejaculate]. *Ukr Biokhim Zh (1978)* (1993) 65(4):64–70.

52. Byrd W, Wolf DP. Acrosomal status in fresh and capacitated human ejaculated sperm. *Biol Reprod* (1986) 34(5):859–69. doi: 10.1095/biolreprod34.5.859

53. Fanani ML, Maggio B. The many faces (and phases) of ceramide and sphingomyelin I - single lipids. *Biophys Rev* (2017) 9(5):589–600. doi: 10.1007/s12551-017-0297-z

54. Zanetti SR, Monclus Mde L, Rensetti DE, Fornes MW, Aveldano MI. Differential involvement of rat sperm choline glycerophospholipids and sphingomyelin in capacitation and the acrosomal reaction. *Biochimie* (2010) 92(12):1886–94. doi: 10.1016/j.biochi.2010.08.015

55. Cross NL. Sphingomyelin modulates capacitation of human sperm. *vitro Biol Reprod* (2000) 63(4):1129–34. doi: 10.1095/biolreprod63.4.1129

56. Blunsom NJ, Cockcroft S. CDP-diacylglycerol synthases (CDS): gateway to phosphatidylinositol and cardiolipin synthesis. *Front Cell Dev Biol* (2020) 8:63. doi: 10.3389/fcell.2020.00063

57. Carrasco E, Casper D, Werner P. PGE(2) receptor EP1 renders dopaminergic neurons selectively vulnerable to low-level oxidative stress and direct PGE(2) neurotoxicity. *J Neurosci Res* (2007) 85(14):3109–17. doi: 10.1002/jnr.21425

58. Roy AC, Ratnam SS. Biosynthesis of prostaglandins by human spermatozoa in *vitro* and their role in acrosome reaction and fertilization. *Mol Reprod Dev* (1992) 33 (3):303–6. doi: 10.1002/mrd.1080330311

59. Docherty JC, Wilson TW. Indomethacin increases the formation of lipoxygenase products in calcium ionophore stimulated human neutrophils. *Biochem Biophys Res Commun* (1987) 148(2):534–8. doi: 10.1016/0006-291x(87)90909-0

60. Mack SR, Han HL, De Jonge J, Anderson RA, Zaneveld LJ. The human sperm acrosome reaction does not depend on arachidonic acid metabolism via the cyclooxygenase and lipoxygenase pathways. *J Androl* (1992) 13(6):551–9. doi: 10.1002/j.1939-4640.1992.tb00351.x

61. Guo H, Li X, Zhang Y, Li J, Yang J, Jiang H, et al. Metabolic characteristics related to the hazardous effects of environmental arsenic on humans: A metabolomic review. *Ecotoxicol Environ Saf* (2022) 236:113459. doi: 10.1016/j.ecoenv.2022.113459

62. Cialdella-Kam L, Nieman DC, Sha W, Meaney MP, Knab AM, Shanely RA. Dose-response to 3 months of quercetin-containing supplements on metabolite and quercetin conjugate profile in adults. *Br J Nutr* (2013) 109(11):1923–33. doi: 10.1017/S0007114512003972

63. Lu D, Yang F, Lin Z, Zhuo J, Liu P, Cen B, et al. A prognostic fingerprint in liver transplantation for hepatocellular carcinoma based on plasma metabolomics profiling. *Eur J Surg Oncol* (2019) 45(12):2347–52. doi: 10.1016/j.ejso.2019.07.004

64. Gatius S, Jove M, Megino-Luque C, Alberti-Valls M, Yeramian A, Bonifaci N, et al. Metabolomic analysis points to bioactive lipid species and acireductone dioxygenase 1 (ADI1) as potential therapeutic targets in poor prognosis endometrial cancer. *Cancers (Basel)* (2022) 14(12). doi: 10.3390/cancers14122842

65. Wu Y, Ding R, Zhang X, Zhang J, Huang Q, Liu L, et al. Meet-in-metabolite analysis: A novel strategy to identify connections between arsenic exposure and male infertility. *Environ Int* (2021) 147:106360. doi: 10.1016/j.envint.2020.106360